

Article

Provenance and Stratigraphy of the Upper Carboniferous—Lower Permian Strata of October Revolution Island (Severnaya Zemlya Archipelago): Implications for Geological History of the Russian High Arctic

Victoria Ershova ^{1,2,3,*} , Andrei Prokopiev ³, Daniel Stockli ⁴, Daria Zbukova ⁵ and Anton Shmanyak ⁵¹ Institute of Earth Science, St. Petersburg State University, University Nab. 7/9, St. Petersburg 199034, Russia² Geological Institute, Russian Academy of Sciences, Pyzhevski Lane 7, Moscow 119017, Russia³ Diamond and Precious Metal Geology Institute, Siberian Branch, Russian Academy of Sciences, Lenin Av. 39, Yakutsk 677980, Russia⁴ Jackson School of Geoscience, University of Texas at Austin, Austin, TX 78712-1692, USA⁵ All Russian Geological Institute, Sredniy Prospect 39, St. Petersburg 199034, Russia

* Correspondence: v.ershova@spbu.ru



Citation: Ershova, V.; Prokopiev, A.; Stockli, D.; Zbukova, D.; Shmanyak, A. Provenance and Stratigraphy of the Upper Carboniferous—Lower Permian Strata of October Revolution Island (Severnaya Zemlya Archipelago): Implications for Geological History of the Russian High Arctic. *Minerals* **2022**, *12*, 1325. <https://doi.org/10.3390/min12101325>

Academic Editor: Yamirka Rojas-Agramonte

Received: 7 September 2022

Accepted: 11 October 2022

Published: 20 October 2022

Publisher's Note: MDPI stays neutral with regard to jurisdictional claims in published maps and institutional affiliations.



Copyright: © 2022 by the authors. Licensee MDPI, Basel, Switzerland. This article is an open access article distributed under the terms and conditions of the Creative Commons Attribution (CC BY) license (<https://creativecommons.org/licenses/by/4.0/>).

Abstract: Small depressions across the north-eastern part of October Revolution Island (Severnaya Zemlya archipelago, Kara terrane) are filled with continental terrigenous rocks, dated as Upper Carboniferous–Lower Permian in age based on palynological data. These rocks overlie Ordovician volcanoclastic rocks above a prominent angular unconformity. U-Pb dating of detrital zircons from the Late Carboniferous–Lower Permian rocks reveals that most grains are Ordovician in age, ranging between 475–455 Ma. A subordinate population of Silurian detrital zircons is also present, contributing up to 15% of the dated population, while Precambrian grains mainly yield Neo-Mesoproterozoic ages and do not form prominent peaks. The combined U-Pb and (U-Th)/He ages indicate that most zircon (U-Th)/He ages were reset and average at ca. 317 Ma, suggesting ~6–7 km of Late Carboniferous uplift within the provenance area. This provenance area, mainly comprising Ordovician magmatic and volcanic rocks, was located close to the study area based on the coarse-grained nature of Late Carboniferous–Lower Permian rocks of north-eastern October Revolution Island. Therefore, we propose that Late Paleozoic tectonism significantly affected both the southern margin of the Kara terrane, as previously supposed, and also its north-eastern part. We propose that the Late Paleozoic Uralian suture zone continued to the north-eastern October Revolution Island and was responsible for the significant tectonic uplift of the studied region. This suture zone is now hidden beneath the younger Arctic basins.

Keywords: geochronology; U-Pb dating; Late Paleozoic; Arctic; Kara Sea

1. Introduction

The Arctic realm is becoming an increasingly popular region for geological research due to its potential mineral and hydrocarbon prospectivity. However, geological studies across this frontier region are severely hampered by its inherent remoteness and severe weather conditions. Furthermore, the majority of the Arctic realm is covered by shallow seas. Numerous deep wells have been drilled in the offshore Norwegian, Canadian, and American sectors, providing important constraints on the offshore stratigraphy. However, in the Russian sector, deep wells have only been drilled offshore in the Barents Sea basin, with no deep wells drilled in the Kara, Laptev, or East Siberian seas. Consequently, insights into the geological structure and geodynamic evolution of the eastern Russian Arctic can only be obtained from the detailed studies of limited onshore outcrops on the island archipelagoes and coastal areas. A critical area for understanding the geological evolution of the Kara and Laptev Sea regions is the Severnaya Zemlya archipelago, representing

a natural land border between these two shallow seas. The archipelago comprises the Pioneer, October Revolution, Komsomolets, and Bol'shevik islands, along with a few other small island groups (Figure 1). Severnaya Zemlya represents the exposed part of the so-called Kara terrane (North Kara terrane, North Kara Basin), which also comprises a significant part of the Kara Sea shelf and the northern part of the Taimyr Peninsula [1–4]. The Kara terrane is separated from the Siberian craton by a major Late Paleozoic suture zone, which can be traced offshore to the west beneath the Kara Sea and West Siberian Basin (Figure 1). However, there is a few different models of continuation Uralian suture from the onshore to the offshore region and further to the east [5–7]. The recent low-temperature studies [8] claimed that the southern part of Kara terrane was affected by the Late Paleozoic uplift caused by the Uralian ocean closure. Furthermore, based on low-temperature thermochronology it was assumed that the western part of Kara terrane was not affected by significant uplift and deformation in Late Paleozoic [3]. The northern and eastern margins of Kara terrane abut onto the Cenozoic Eurasia oceanic basin and further continuation of Late Paleozoic deformation are debatable. Therefore, rocks exposed across the Severnaya Zemlya archipelago can be used to reconstruct the Paleozoic history of the Kara terrane and adjacent parts of the Arctic. Previous provenance studies from the Severnaya Zemlya archipelago, mainly focusing on U-Pb dating of detrital zircons from Cambrian–Devonian strata [1,3,9–11], suggest that the major source of clastic detritus shifted from the Timanian orogeny during the earliest Paleozoic to the Caledonian orogeny during the Middle Paleozoic. In comparison to Cambrian–Devonian strata, the Carboniferous–Permian rocks of Severnaya Zemlya are still poorly studied. The Upper Paleozoic deposits have only been studied on Bol'shevik Island, where Ershova et al. (2015) [10] suggested a local provenance area for Carboniferous–Permian clastics. Here, we present the first biostratigraphy and provenance study for Carboniferous–Permian deposits of north-eastern October Revolution Island and aim to improve our understanding of the Late Paleozoic history of Kara terrane and adjacent Arctic region.

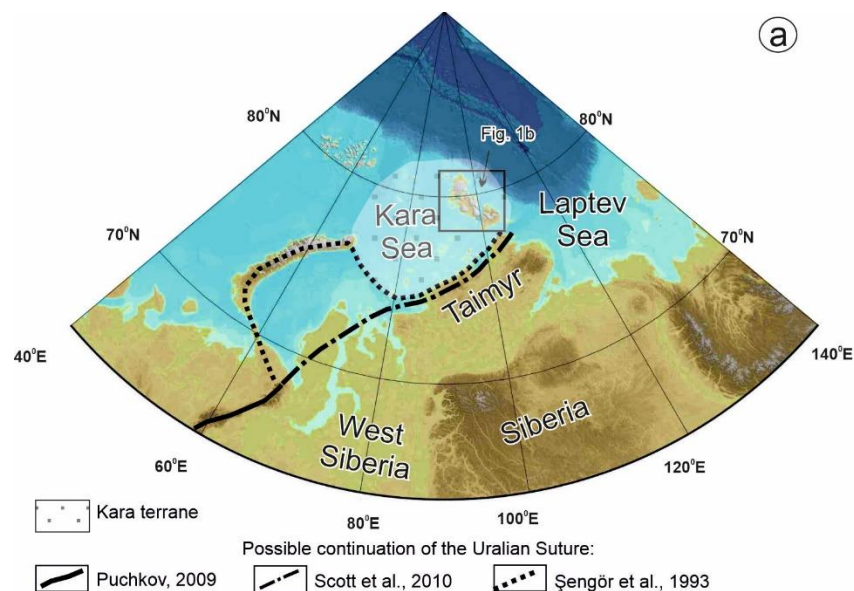


Figure 1. Cont.

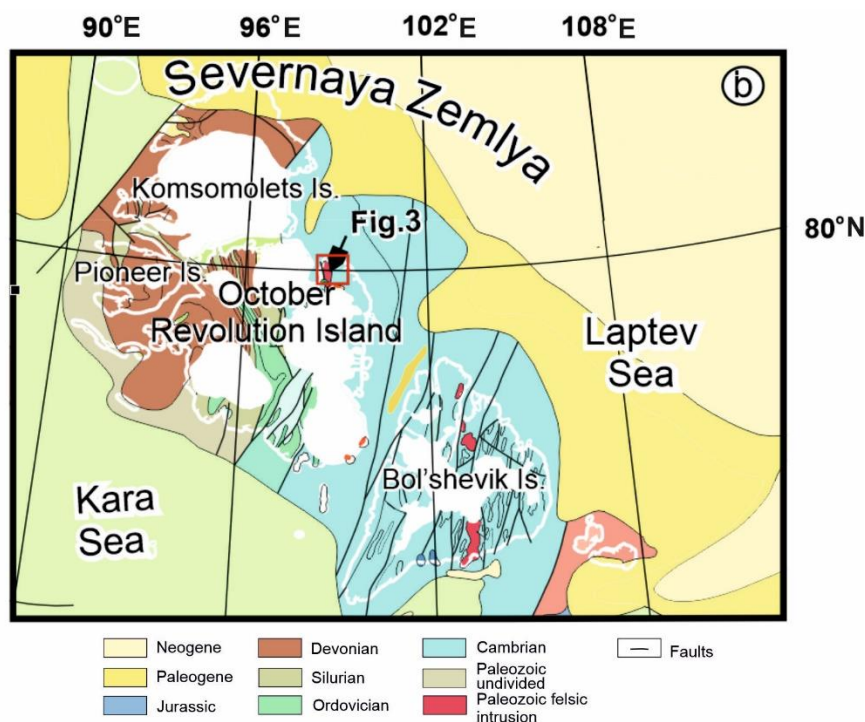


Figure 1. (a) Location of the study area [5–7]; (b) Simplified geological map of the Severnaya Zemlya archipelago (modified after [12,13]).

2. Geological Background

The Severnaya Zemlya archipelago comprises a Cambrian to Permian sedimentary succession (Figure 1) [2,12,14] and references therein. The October Revolution, Pioneer, and Komsomolets islands are mainly composed of Cambrian to Upper Devonian sedimentary rocks, while Carboniferous and Permian strata have a patchier distribution (Figures 1 and 2). Bol'shevik Island is mainly composed of Cambrian–Ordovician rocks, with local occurrences of Devonian, Upper Carboniferous–Permian and Mesozoic clastic rocks [12,14]. The geological structure of the archipelago is characterized by a major NW-SE-trending anticline, located in the central part of October Revolution Island [1]. Lower and Middle Ordovician, disharmonically folded, evaporite-bearing strata are exposed in the core of this anticline, while Upper Ordovician to Silurian clastic and carbonate rocks outcrop on its limbs.

Several generations of Paleozoic granitic intrusions are reported from the Severnaya Zemlya archipelago. The first major episode of magmatic activity occurred during the latest Cambrian–Ordovician, with volcanic rocks yielding ages between 491 and 482 Ma, while plagiogranites reported from the central and southern parts of October Revolution Island yield ages of 488–474 Ma [1]. Kurapov et al. (2020) [15] report that granitic intrusions from the eastern part of October Revolution Island yield Sandbian (ca. 457 Ma) crystallization ages.

The second episode of granitic magmatism has been dated as Early Carboniferous, based on two granitic intrusions from Bol'shevik Island yielding U-Pb zircon ages of 342.0 ± 3.6 and 343.5 ± 4.1 Ma [16].

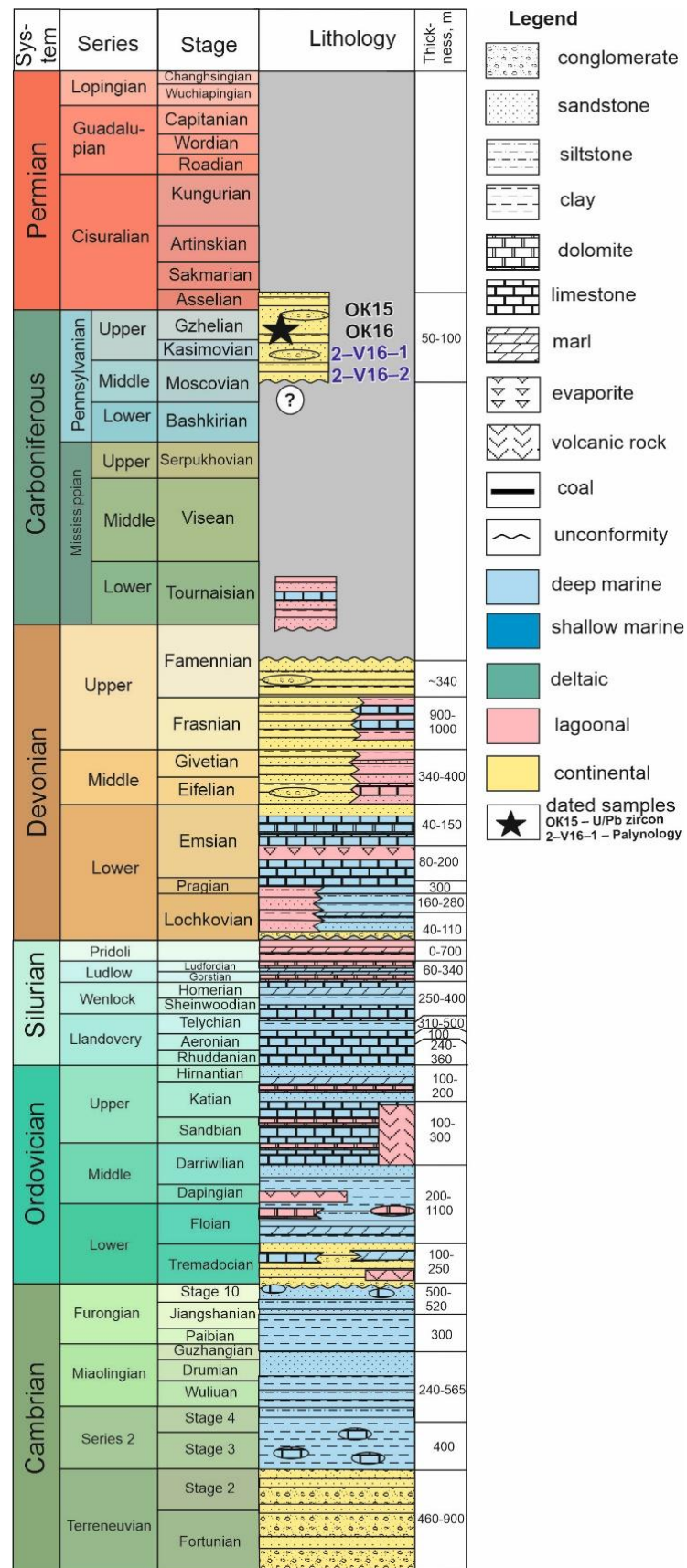


Figure 2. Simplified stratigraphic column of the Paleozoic strata of Severnaya Zemlya archipelago (modified after [12]).

3. Geological Setting of Study Area and Position of Studied Samples

The northeastern part of October Revolution Island comprises intensely deformed Lower Cambrian and Lower Ordovician deposits (Figure 3). Cambrian rocks are represented by intercalated siltstones, sandstones, and argillites, with subordinate beds of limestone. Lower Ordovician rocks comprise tuffs, volcanoclastic rocks, and felsic intrusions. Mafic intrusions are subordinate but presumably also Ordovician in age [17].

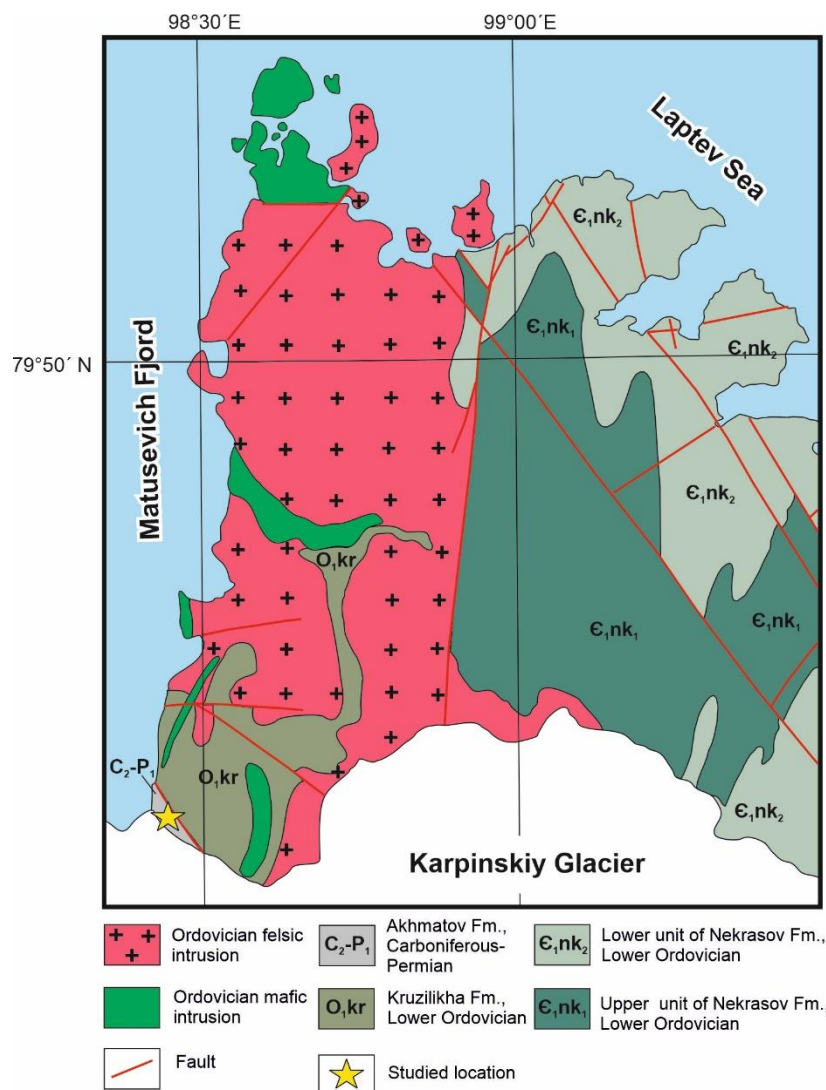


Figure 3. Geological map of the study area and location of samples (modified after [14,17]).

Samples were collected from exposures along the south-eastern coast of Matusevich Fjord (Figure 3), where two rock units of contrasting ages and structural styles crop out.

Lower Ordovician volcanoclastic deposits form a steeply dipping monocline, comprising tuffaceous mudstones and siltstones with subordinate interlayers of felsic tuffs, mafic tuffs, and volcanic rocks (Figure 4). Tuffaceous mudstones and siltstones are cherry and bright green in color, medium-platy and massive, with individual beds attaining a thickness of 0.2–1.5 m. Interlayers of pinkish-beige tuffs and rhyolites occur, which attain thicknesses of up to 0.7 m. Subordinate beds of dark gray-green and bright green andesite ranging from 0.2–0.8 m in thickness have also been reported. Several hundred meters of Lower Ordovician rocks are exposed under the edge of the Karpinskiy glacier.

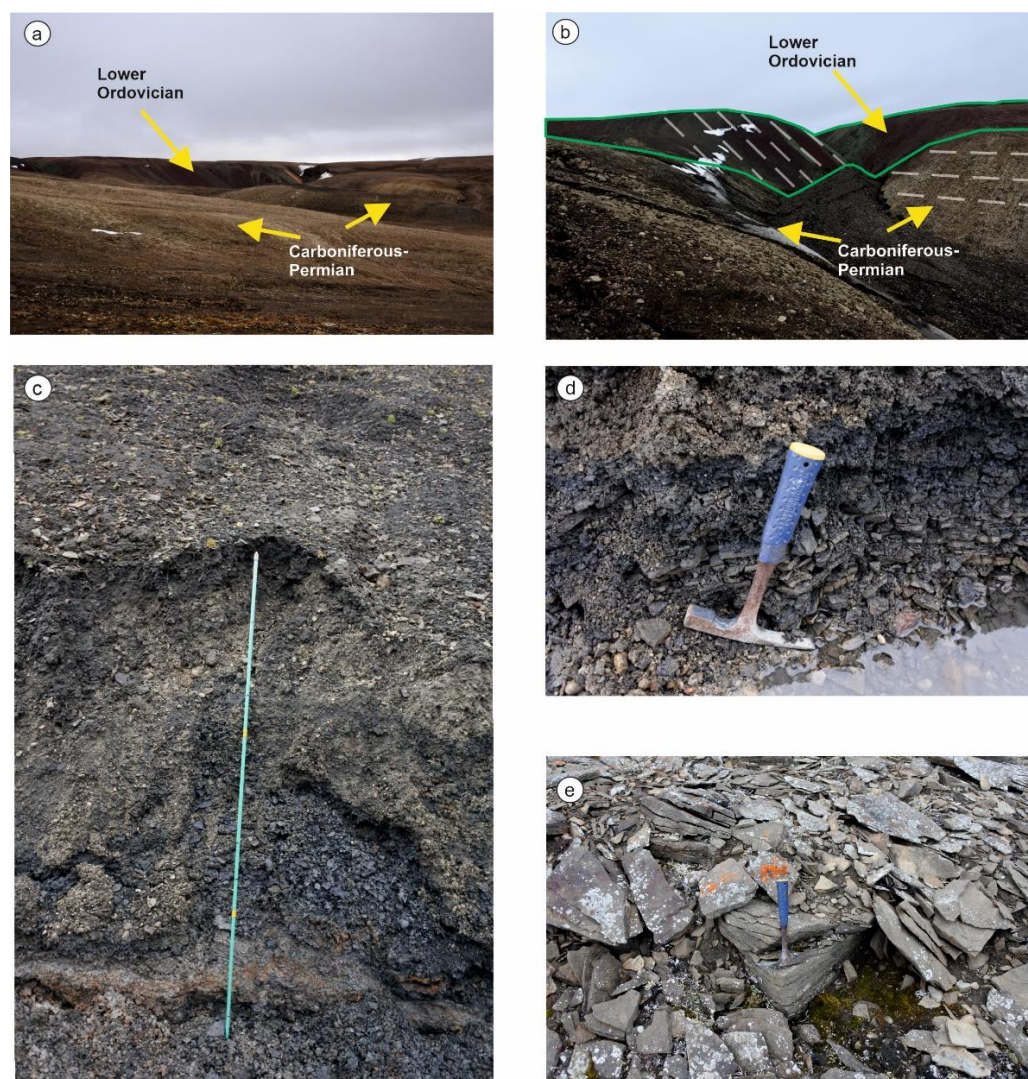


Figure 4. Field photographs of studied Carboniferous–Permian deposits: (a)—General view of the study area, (b)—close up view of the relationship between Lower Ordovician and Upper Paleozoic deposits, (c)—general view of an outcrop of Carboniferous–Permian deposits, (d)—intercalated sandstones and siltstones with layers of coal, (e)—cross-bedded sandstones.

Lower Ordovician deposits are overlain by Carboniferous–Permian terrigenous rocks. The contact between the Ordovician and Upper Paleozoic deposits is covered by talus in all outcrops across the studied area and cannot be observed. However, Ordovician deposits form a steeply dipping monocline, while Upper Paleozoic rocks lie either horizontally or form a gentle monocline. These differences in structural styles support the existence of an angular unconformity between the Ordovician and Carboniferous–Permian sedimentary units. Moreover, it is likely that Carboniferous–Permian sediments were deposited in paleo-depressions developed on an irregular basement of deformed Ordovician rocks, which exhibited considerable variation in topography (Figure 4a,b). Carboniferous–Permian rocks are poorly exposed and probably smoothed out by glacial erosion but form small ridges cut by the valleys of modern streams. Upper Paleozoic deposits comprise exclusively terrigenous rocks. The main part of the section is composed of intercalating siltstones and clays, ranging from light gray to almost black in color, with subordinate coaly units. Sandstone beds with interlayers of polymictic gravelstones and conglomerates are found within the succession. Sandstones are predominantly medium- to coarse-grained, polymictic in composition, massive, and locally cross-bedded. Although the exposure is very poor, it appears that sandstone and conglomerate interlayers are laterally discontinuous. The

occurrence of carbonaceous interlayers and coal suggests that the deposits are continental and most likely alluvial in origin, with the laterally discontinuous sandstone and conglomerate beds representing channel facies. These strata in the local stratigraphic scheme attributed to Akhmatov Formation and based on fossiliferous flora were considered as Late Carboniferous-Early Permian in age [14].

4. Palynology

Samples were prepared following standard techniques including demineralization of the rock matrix using hydrochloric and hydrofluoric acids, sample dispersion by adding an aqueous solution of caustic alkali, sample separation in a centrifuge with a heavy liquid, and release from fine mineral and amorphous organic particles using an ultrasonic bath and a synthetic sieve with a mesh size of 10 microns. Microscopic examination was carried out at 400 times magnification. As a result, the following data were obtained.

Two samples of shales were studied for palynological analysis. Both samples contain numerous spore and pollen grains, totaling 203 grains in sample 2-V16-1 and 170 grains in sample 2-V16-2, respectively. The results of the palynological analysis are summarized in Table 1 and Supplementary S1.

Table 1. List of spore and pollen from studied deposits.

#	Species	Number of Grains	
		2-V16-1	2-V16-2
Spores			
1.	<i>Calamospora</i> sp.	-	6
2.	cf. <i>C.</i> sp.	4	-
3.	<i>Leiotriletes</i> sp.	3	5
4.	<i>Punctatisporites</i> aff. <i>barakarensis</i> (Bharad. et Sriv.) Oshurk.	1	-
5.	<i>P. labiosus</i> Virv.	5	3
6.	<i>P. orbicularis</i> Kos.	-	11
7.	<i>P. planus</i> Verb.	6	-
8.	<i>P. sublaevis</i> (Inoss.) Oshurk.	-	3
9.	<i>P.</i> sp.	7	-
10.	<i>P.</i> cf. sp.	-	4
11.	<i>Trachitriletes asper</i> Isch.	1	-
12.	<i>T.</i> sp.	2	-
13.	<i>Bifurcatisporites bifurcatus</i> (Kalibova) Inoss.	-	3
14.	<i>Retusotriletes lemniscatus</i> (Lub.) Pashk.	5	7
15.	<i>Chanovejisorites confluens</i> (S.Arch. et Gam.) Oshurk.	2	3
16.	<i>C.</i> aff. <i>versus</i> (Price) Oshurk.	2	-
17.	<i>C.</i> sp.	12	-
18.	<i>Schopfites colchesterensis</i> Kos.	29	40
19.	<i>S. dimorphus</i> Kos.	53	21
20.	cf. <i>S. dimorphus</i> Kos.	4	-
21.	<i>Horriditriletes trichacanthus</i> (Lub.) Oshurk.	10	-
22.	<i>Spinosisporites hirsutus</i> Inoss.	-	2
23.	<i>Acanthotriletes rectispinus</i> (Lub.) Isch.	-	6
24.	<i>Iugisporis circumactus</i> (Isch.) Oshurk.	3	-

Table 1. Cont.

#	Species	Number of Grains	
		2-V16-1	2-V16-2
Spores			
25.	<i>Reticulatisporites calamistratus</i> (Isch.) Oshurk.	-	3
26.	<i>R. contortoreticulatus</i> (Sadk.) Drjag.	4	-
27.	<i>Microreticulatisporites comulatus</i> (Isch.) Oshurk.	-	4
28.	<i>Periplecotriletes crassus</i> Isch.	2	1
29.	<i>P. intricatus</i> (Lub.) Oshurk.	-	2
30.	<i>Foveolatisporites perforatus</i> Inoss.	-	4
31.	<i>F. quaesitus</i> (Kos.) Bharad.	5	-
32.	<i>Cadiospora crypta</i> Turn.	2	1
33.	<i>C. sp.</i>	2	-
34.	<i>Crassispora echinata</i> Tet. et Shwarts.	7	27
35.	<i>Callisporites cingulatus</i> (Alpern) Shwarts.	1	2
36.	<i>Densosporites reynoldsburgensis</i> Kos.	2	1
37.	<i>Psilohymena psiloptera</i> (Lub.) Hart et Harr.	3	-
38.	<i>Lycospora sp.</i>	-	5
39.	<i>Endosporites sp.</i>	3	-
40.	<i>Remysporites magnificus</i> (Horst) Butt. et Will.	1	-
Pollen			
1	<i>Guthoerlisporites cancellosus</i> Playf. et Dett.	1	-
2	cf. <i>G. rugosus</i> Inoss.	1	-
3	<i>Florinites antiquus</i> S.W. et B.	2	2
4	<i>F. macropterus</i> (Lub.) Dibn.	2	9
5	<i>F. pumicosus</i> (Ibr.) S. W. et B.	1	-
6	<i>Cordaitina rotata</i> (Lub.) Samoil.	4	-
7	<i>C. cf. rotata</i> (Lub.) Samoil.	-	1
8	<i>Bascanisporites sp. aff. undosus</i> Balme et Hennelly	1	-
9	cf. <i>B. sp.</i>	1	-
10	<i>Samoilovitchisaccites cf. turboreticulatus</i> (Samoil.) Dibn.	1	-
11	<i>Illinites elegans</i> Kos.	2	-
12	<i>Vestigisporites sp.</i>	2	-
13	<i>Protochaploxypinus sp.</i>	1	-
14	<i>Striatoabieites sp. aff. parvisaccus</i> (Efr.) Oshurk.	2	-
15	<i>Striatopodocarpites cancellatus</i> (B.et H.) Hart	1	-
Total:		203	170

∴ This means that there is no this pollen in the sample.

Both samples contain numerous species, including are typical for Middle–Upper Carboniferous strata: *Punctatisporites orbicularis* Kos., *Retusotriletes lemniscatus* (Lub.) Pashk., *Schopfites colchesterensis* Kos., *S. dimorphus* Kos., cf. *S. dimorphus* Kos., *Foveolatisporites quaesitus* (Kos.) Bharad., *Densosporites reynoldsburgensis* Kos., *Remysporites magnificus* (Horst) Butt. et Will., *Florinites antiquus* S.W. et B., *Illinites elegans* Kos. and Upper Carboniferous: *Horriditriletes trichacanthus* (Lub.) Oshurk., *Reticulatisporites contortoreticulatus* (Sadk.) Dr-

jag., *Crassispora echinata* Tet. et Shwarts., *Psilohymena psiloptera* (Lub.) Hart et Harr., and cf. *Guthoerlisporites rugosus* Inoss. (Table 1). This assemblage is comparable to the Late Carboniferous assemblage identified by R. Kosanke from the Pennsylvania Illinois Coal Basin [18].

However, the samples also contain subordinate species which are typical for the Late Carboniferous and Early Permian palynological assemblages identified by various researchers in the Pechora and Kuznetsk basins of Russia, Kazakhstan, and Australia [19–24], including *Punctatisporites sublaevis* (Inoss.) Oshurk., *Bifurcatisporites bifurcatus* (Kalibova) Inoss., *Chanovejisporites confluens* (S.Arch. et Gam.) Oshurk., *C. sp.*, *Spinosisporites hirsutus* Inoss., *Cadiospora crypta* Turn., *Callisporites cingulatus* (Alpern) Shwarts., *Florinites pumicosus* (Ibr.) S., W. et B., cf. *Bascanisporites sp.*, *Vestigisporites sp.*, and Lower Permian: *Punctatisporites aff. barakarensis* (Bharad. et Sriv.) Oshurk., *P. labiosus* Virb., *P. planus* Virb., *Chanovejisporites aff. versus* (Price) Oshurk., *Acanthotriletes rectispinus* (Lub.) Isch., *Guthoerlisporites cancellosus* Playf. et Dett., *Cordaitina rotata* (Lub.) Samoil., *C. cf. rotata* (Lub.) Samoil., *Bascanisporites sp. aff. undosus* Balme et Hennelly, *Samoilovitchisaccites cf. turboreticulatus* (Samoil.) Dibr., *Striatoabieites sp. aff. parvisaccus* (Efr.) Oshurk., and *Striatopodocarpites cancellatus* (B. et H.) Hart.

Therefore, the studied terrigenous deposits from north-eastern October Revolution Island can be assigned a Late Carboniferous–Early Permian age based on their spore and pollen assemblage.

5. U-Pb and (U-Th)/He Dating of Detrital Zircons

5.1. Methods

Samples were analyzed for detrital zircon U-Pb ages at the UTChron geochronology facility in the Department of Geological Sciences at the University of Texas, Austin. Samples underwent conventional heavy mineral separation and were grain mounted (no polishing) on one-inch round epoxy pucks with double-sided tape. All grains were depth-profiled using a Photon Machines Analyte G2 ATLex 300si ArF 193 nm Excimer Laser, equipped with a Helix two-volume ablation cell. The ablated aerosols were transported using He gas to, and analyzed with, a Thermo Fisher Element2 single collector, magnetic sector-ICP-MS. $^{206}\text{Pb}/^{238}\text{U}$ ages are reported for grains that are younger than 1000 Ma. The histogram was constructed using the detzrcr software [25].

Detrital zircon (U-Th)/He (ZHe) analyses were performed to provide additional geochronologic constraints. Specific grains that were at least 70 μm in diameter were chosen, and they appeared to have few, if any, visible inclusions. Analyses were conducted following the analytical procedures described in [26]. All ages were corrected for the effects of α -ejection [27] and are reported with a $\sim 8\%$ (2σ) analytical uncertainty. The data tables are presented in Supplementary S2 and Supplementary Table S3.

5.2. U-Pb and (U-Th)/He Dating Results

5.2.1. U-Pb Dating

Sample Ok15 (medium to coarse-grained lithic arenite). Precambrian and Cambrian zircons (5%) do not form any prominent peaks. The sample yielded one Mesoproterozoic and Cambrian grains and four latest Neoproterozoic. Ordovician grains are predominant (84%) forming a peak at 465 Ma. Silurian grains (10%) are early-middle Silurian in age and do not form prominent peaks. The single Devonian grain is the youngest within a dated population (371 ± 7.5 Ma) (Figure 5a).

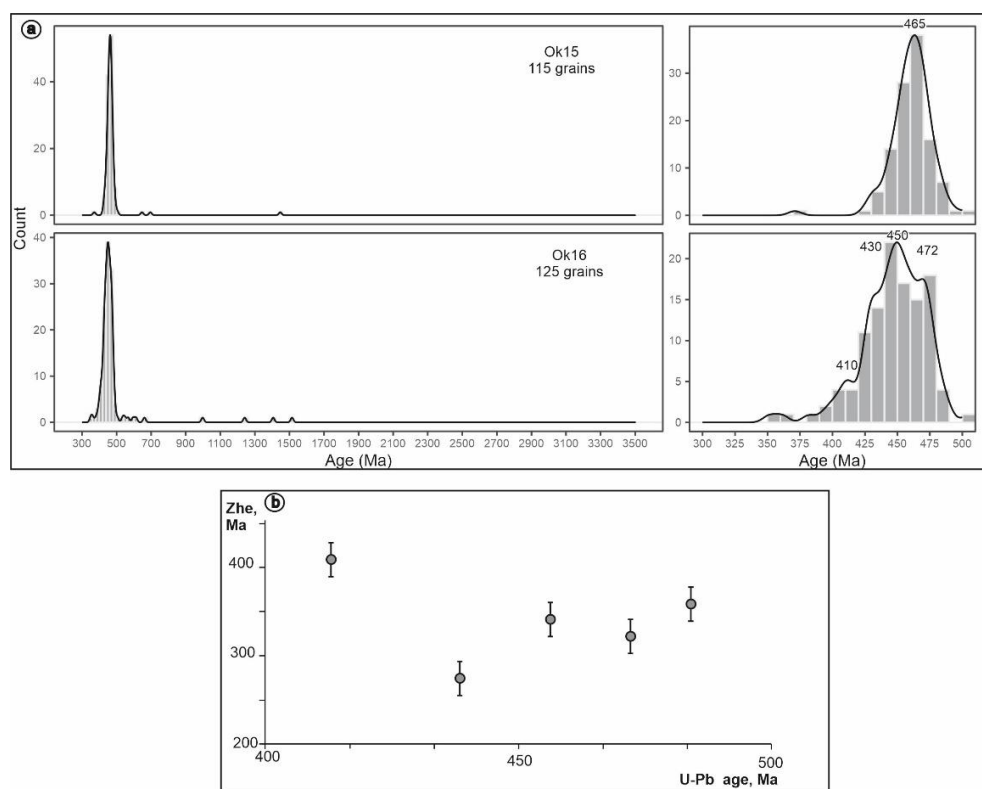


Figure 5. Kernel Density Estimation (KDE) plots depicting the U-Pb detrital zircon data (a,b) double-dated (U-Pb and (U-Th)/He) zircons from the Upper Carboniferous–Lower Permian strata of north-eastern October Revolution Island.

Sample Ok16 (medium to coarse-grained lithic arenite). Precambrian zircons (7%) are Mesoproterozoic and Latest Neoproterozoic in age, while Cambrian grains (3%), both populations do not form prominent peaks. Ordovician zircons (54%) are a prevailing group at ca. 472 and 450 Ma. Silurian grains (26%) form peak at ca. 430 Ma. Devonian zircons (10%) group at subordinate peak at 410 Ma. The two Carboniferous zircons do not form a prominent peak with the youngest grain yielding 351.5 ± 5.3 Ma age (Figure 5a).

5.2.2. U-Pb and (U-Th)/He Dating

The combined U-Pb and (U-Th)/He dating results are depicted in Figure 5b. (U-Th)/He ages range between 414.7 ± 33.18 and 273.0 ± 21.84 . The grain with a (U-Th)/He ages of 414.7 Ma yielded a U-Pb crystallization age of 413.0 ± 7.2 Ma, suggesting that the (U-Th)/He system of this grain has not been reset (Figure 5b). However, other grains with Ordovician to earliest Silurian U-Pb crystallization ages yielded Late Paleozoic (U-Th)/He ages averaging at ca. 317 Ma, indicating that the (U-Th)/He system of most zircons has been reset.

6. Discussion

The studied clastics unconformably overlie Lower Ordovician volcanoclastic rocks and were deposited in a continental alluvial environment within a small depression across north-eastern October Revolution Island. Palynological analyses suggest that they are Late Carboniferous–Early Permian in age.

The unimodal distribution of detrital zircons, with the majority of grains yielding ages spanning 475–455 Ma, suggests that Ordovician felsic magmatic rocks were the main provenance for Upper Paleozoic continental clastics widely occurred across the north-eastern October Revolution Island [14,17]. Minor populations of the latest Neoproterozoic

and Silurian detrital zircons may have been reworked from older Paleozoic strata of the Severnaya Zemlya archipelago, where they are numerous (Figure 6).

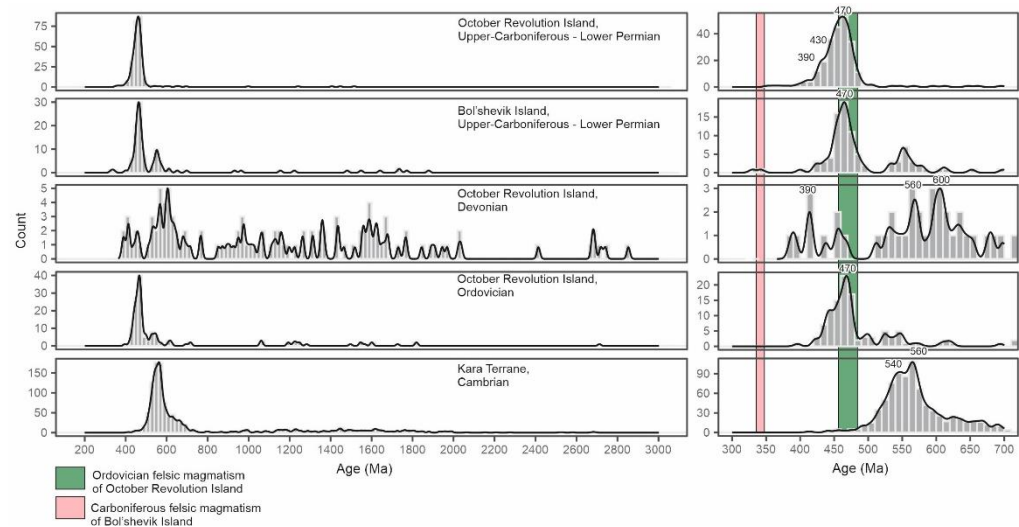


Figure 6. Comparison of detrital zircon age spectra (KDE plots) from Paleozoic strata of the Kara terrane (this study and [2,10,11]). Ages of magmatic events from [15,16].

The combined (U-Th)/He and U-Pb dating of zircons indicates that most zircon ages were reset in the Carboniferous, defining the main exhumation and cooling event in the source region (Figure 5b). Late Paleozoic (U-Th)/He zircon ages average at ca. 317 Ma, determining the timing of major uplift across the provenance area. A proximal provenance is likely due to the coarse-grained nature of the studied clastics, suggesting that the north-eastern margin of the Severnaya Zemlya archipelago experienced significant Late Paleozoic tectonism and uplift. However, our data contrast with data from the western part of the archipelago, where (U-Th)/He zircon ages from Ordovician–Devonian strata were not reset during the Carboniferous–Permian, yielding Early–Middle Paleozoic exhumation ages [3]. The only known magmatic intrusions of the Carboniferous age within the archipelago are the Early Carboniferous intrusions on Bol'shevik Island [16]. However, northern Taimyr represented the long-lived Late Paleozoic active southern margin of the Kara terrane, containing major pulses of magmatic and tectonic activity at 316 and 299 Ma [28,29]. These dates correlate well with the timing of uplift revealed by our data from north-eastern October Revolution Island, suggesting that coeval tectonism and uplift also occurred in this region. By contrast, previous researchers assumed that Late Paleozoic deformations were restricted to a narrow zone along the south-eastern margin of the Kara terrane, proposing an oblique style of collision with predominantly strike-slip displacement [8].

Our new data suggest that coeval Late Paleozoic tectonism significantly affected both the southern margin of the Kara terrane, as previously assumed, and also the north-eastern margin (modern coordinates). Based on the closure of (U-Th)/He zircon ages [27], a Late Carboniferous uplift of as much as 5–6 km occurred across the study area. Long-lived Late Paleozoic magmatism of the Kara terrane has been recently interpreted as representing the active margin of the Uralian ocean [28,29], allowing us to propose that the Late Paleozoic suture zone continued eastward to north-eastern October Revolution Island and was responsible for significant tectonic uplift of the study region. This suture zone is now hidden beneath the younger oceanic Arctic basins.

7. Conclusions

- (1) The studied clastics deposited in a continental environment within a small depression across north-eastern October Revolution Island. Palynological analyses showed that they are Late Carboniferous–Early Permian in age.

- (2) U-Pb dating of detrital zircon revealed that most grains yielding Early Paleozoic ages spanning 475–455 Ma are predominant within the dated samples. Silurian zircons comprise the second largest population, contributing up to 26% of the dated grains. The few Neoproterozoic grains span 570–700 Ma, Mesoproterozoic grains range in age between 1240 and 1515 Ma, while Devonian–Early Carboniferous zircons (~5%) span 351–382 Ma. Thus, the almost unimodal distribution of detrital zircons claims Ordovician volcanic and magmatic rocks as the predominant provenance area for studied clastics. Silurian-Devonian terrigenous rocks are the subordinate source of clastic grains.
- (3) The combined (U-Th)/He and U-Pb dating of zircons indicates that most zircon ages were reset in the Carboniferous, defining the main exhumation and cooling event in the provenance area.
- (4) Our new data suggest that coeval Late Paleozoic tectonism significantly affected the north-eastern margin of Kara terrane than was assumed previously. We propose that the Late Paleozoic suture zone of the Uralian Ocean is located close to the study region and now is hidden under the young Arctic ocean.

Supplementary Materials: The following are available online at <https://www.mdpi.com/article/10.3390/min12101325/s1>, Supplementary S1, Supplementary S2, and Supplementary S3.

Author Contributions: V.E. investigation, writing—original draft preparation; A.P.—investigation, writing, and editing; D.S. investigation; D.Z.—investigation, A.S.—investigation. All authors have read and agreed to the published version of the manuscript.

Funding: Interpretation of isotopic data and tectonics were supported by the Russian Science Foundation (grant No. 20-17-00169); basic funding of AP through a subsidy of DPMGI SB RAS, VE and DS were supported by NOR-R-AM2 No. 309477.

Data Availability Statement: Not applicable.

Acknowledgments: This work was supported by the project “Changes at the Top of the World through Volcanism and Plate Tectonics: A Norwegian-Russian-North American collaboration in Arctic research and education” (NOR-R-AM2) No. 309477. Interpretation of isotopic study and correlation with Taimyr-Severnaya Zemlya were supported by RSF grant 20-17-00169. Basic funding of AP through a subsidy of DPMGI SB RAS. We are grateful to James Barnet for correcting the English.

Conflicts of Interest: The authors declare no conflict of interest.

References

1. Lorenz, H.; Gee, D.G.; Simonetti, A. Detrital zircon ages and provenance of the late Neoproterozoic and Palaeozoic successions on Severnaya Zemlya, Kara shelf: A tie to Baltica. *Nor. Geol. Tidsskr.* **2008**, *88*, 235–258.
2. Lorenz, H.; Männik, P.; Gee, D.; Proskurnin, V. Geology of the Severnaya Zemlya Archipelago and the North Kara Terrane in the Russian high Arctic. *Int. J. Earth Sci.* **2008**, *97*, 519–547. [[CrossRef](#)]
3. Ershova, V.; Anfinson, O.; Prokopiev, A.; Khudoley, A.; Stockli, D.; Faleide, J.I.; Gaina, C.; Malyshev, N. Detrital zircon (U-Th)/He ages from Paleozoic strata of the Severnaya Zemlya Archipelago: Deciphering multiple episodes of Paleozoic tectonic evolution within the Russian High Arctic. *J. Geodyn.* **2018**, *119*, 210–220. [[CrossRef](#)]
4. Metelkin, D.V.; Vernikovskiy, V.A.; Kazansky, A.Y.; Bogolepova, O.K.; Gubanov, A.P. Paleozoic history of the Kara microcontinent and its relation to Siberia and Baltica: Paleomagnetism, paleogeography and tectonics. *Tectonophysics* **2005**, *398*, 225–243. [[CrossRef](#)]
5. Puchkov, V.N. *The Evolution of the Uralian Orogen*; Geological Society; Special Publication: London, UK, 2009; Volume 327, pp. 161–195. [[CrossRef](#)]
6. Scott, R.A.; Howard, J.P.; Guo, L.; Schekoldin, R.; Pease, V. Offset and Curvature of the Novaya Zemlya Fold-and-Thrust Belt, Arctic Russia. *Pet. Geol. Conf. Ser.* **2010**, *7*, 645–657. [[CrossRef](#)]
7. Şengör, A.M.C.; Natal'in, B.A.; Burtman, V.S. Evolution of the Altaid Tectonic Collage and Palaeozoic Crustal Growth in Eurasia. *Nature* **1993**, *364*, 299–307. [[CrossRef](#)]
8. Khudoley, A.K.; Verzhbitsky, V.E.; Zastrozhnov, D.A.; O’Sullivan, P.; Ershova, V.B.; Proskurnin, V.F.; Tuchkova, M.I.; Rogov, M.A.; Kyser, T.K.; Malyshev, S.V.; et al. Late Paleozoic—Mesozoic Tectonic Evolution of the Eastern Taimyr-Severnaya Zemlya Fold and Thrust Belt and Adjoining Yenisey-Khatanga Depression. *J. Geodyn.* **2018**, *119*, 221–241. [[CrossRef](#)]

9. Nikishin, V.A.; Malyshev, N.A.; Nikishin, A.M.; Golovanov, D.Yu.; Proskurnin, V.F.; Soloviev, A.V.; Kulemin, R.F.; Morgunova, E.S.; Ulyanov, G.V.; Fokin, P.A. Recognition of the Cambrian Timan–Severnaya Zemlya Orogen and Timing of Geological Evolution of the North Kara Sedimentary Basin Based on Detrital Zircon Dating. *Dokl. Earth Sci.* **2017**, *473*, 402–405. [[CrossRef](#)]
10. Ershova, V.B.; Prokopiev, A.V.; Nikishin, V.A.; Khudoley, A.K.; Malyshev, N.A.; Nikishin, A.M. New Data on Upper Carboniferous–Lower Permian Deposits of Bol’shevik Island, Severnaya Zemlya Archipelago. *Polar Res.* **2015**, *34*, 24558. [[CrossRef](#)]
11. Ershova, V.B.; Prokopiev, A.V.; Khudoley, A.K.; Andersen, T.; Kullerud, K.; Kolchanov, D.A. U–Pb Age and Hf Isotope Geochemistry of Detrital Zircons from Cambrian Sandstones of the Severnaya Zemlya Archipelago and Northern Taimyr (Russian High Arctic). *Minerals* **2019**, *10*, 36. [[CrossRef](#)]
12. Ershova, V.B.; Prokopiev, A.V.; Khudoley, A.K. Devonian–Permian Sedimentary Basins and Paleogeography of the Eastern Russian Arctic: An Overview. *Tectonophysics* **2016**, *691*, 234–255. [[CrossRef](#)]
13. Morozov, A.F.; Petrov, O.V. *State Geological Map of the Russian Federation. Scale 1:2,500,000*; VSEGEI Publishing House: St. Petersburg, Russia, 2004. (In Russian)
14. Makariev, A.A. (Ed.) *State Geological Map of the Russian Federation. Scale 1:1,000,000 (Third Generation). Sheet T-45—48th. Cheliuskin*; VSEGEI Publishing House: St. Petersburg, Russia, 2012. (In Russian)
15. Kurapov, M.; Ershova, V.; Khudoley, A.; Makariev, A.; Makarieva, E. The First Evidence of Late Ordovician Magmatism of the October Revolution Island (Severnaya Zemlya Archipelago, Russian High Arctic): Geochronology, Geochemistry and Geodynamic Settings. *NJG Nor. J. Geol.* **2020**. [[CrossRef](#)]
16. Lorenz, H.; Gee, D.G.; Whitehouse, M.J. New Geochronological Data on Palaeozoic Igneous Activity and Deformation in the Severnaya Zemlya Archipelago, Russia, and Implications for the Development of the Eurasian Arctic Margin. *Geol. Mag.* **2007**, *144*, 105–125. [[CrossRef](#)]
17. Prokopiev, A.V.; Ershova, V.B.; Sobolev, N.N.; Korago, E.; Petrov, E.; Khudoley, A.K. New data on geochemistry, age and geodynamic settings of felsic and mafic magmatism of the northeastern part of October Revolution Island (Severnaya Zemlya Archipelago). In Proceedings of the AGU Chapman Conference on «Large-Scale Volcanism in the Arctic: The Role of the Mantle and Tectonics», Selfoss, Iceland, 13–18 October 2019; Available online: https://higherlogicdownload.s3.amazonaws.com/AGU/181026d4-2440-440a-a114-8fcd2fc3ada8/UploadedImages/Chapmans/Arctic_Volcanism/ChapmanPresentedAbstracts_ArcticVolcanism.pdf (accessed on 13 October 2019).
18. Kosanke, R.M. Pennsylvanian spores of Illinois and their use in correlation. *Bull. Ill. Geol. Surv.* **1950**, *74*, 128p.
19. Balme, B.E.; Hennelly, J.P.F. Trilete sporomorphs from Australian Permian sediments. *Aust. J. Bot.* **1956**, *4*, 240–260. [[CrossRef](#)]
20. Betekhtina, O.A.; Gorelova, S.G.; Dryagina, L.L.; Danilov, V.I.; Batyaeva, S.P.; Tokareva, P.A. *Upper Paleozoic Rocks of Angarida; Fauna and Flora*; Nauka (Transactions of Institute of Geology and Geophysics of RAS): Novosibirsk, Russia, 1988; 265p.
21. Lyuber, A.A.; Waltz, I.E. Atlas of microspores and pollen of the Paleozoic of the USSR. *Trans. Tr. Vsesofuznogo Nauchno-Issledovatel’skogo Geologicheskogo Inst. Bull.* **1941**, *139*, 108.
22. Oshurkova, M.V. *Morphology, Classification and Description of the Late Paleozoic Myospore Form-Genera*; VSEGEI Publishing House: St. Petersburg, Russia, 2003; 377p.
23. Boronin, V.P.; Burov, B.V. *Paleontological Atlas of the Permian Deposits of the Pechora Coal Basin*; Nauka Publishing House: Leningrad, Russia, 1983; 318p.
24. Oshurkova, M.V.; Panova, L.A.; Romanovskaya, G.M. *Practical Palynostratigraphy*; Nedra: Leningrad, Russia, 1990; 348p.
25. Andersen, T.; Kristoffersen, M.; Elburg, M.A. Visualizing, Interpreting and Comparing Detrital Zircon Age and Hf Isotope Data in Basin Analysis—A Graphical Approach. *Basin Res.* **2018**, *30*, 132–147. [[CrossRef](#)]
26. Wolfe, M.R.; Stockli, D.F. Zircon (U–Th)/He Thermochronometry in the KTB Drill Hole, Germany, and Its Implications for Bulk He Diffusion Kinetics in Zircon. *Earth Planet. Sci. Lett.* **2010**, *295*, 69–82. [[CrossRef](#)]
27. Farley, K.A. (U–Th)/He Dating: Techniques, Calibrations, and Applications. *Rev. Mineral. Geochem.* **2002**, *47*, 819–844. [[CrossRef](#)]
28. Kurapov, M.; Ershova, V.; Khudoley, A.; Luchitskaya, M.; Makariev, A.; Makarieva, E.; Vishnevskaya, I. Late Palaeozoic Magmatism of Northern Taimyr: New Insights into the Tectonic Evolution of the Russian High Arctic. *Int. Geol. Rev.* **2020**, *63*, 1990–2012. [[CrossRef](#)]
29. Kurapov, M.Yu.; Ershova, V.B.; Makariev, A.A.; Makarieva, E.V.; Khudoley, A.K.; Luchitskaya, M.V.; Prokopiev, A.V. Carboniferous Granitoid Magmatism of Northern Taimyr: Results of Isotopic–Geochemical Study and Geodynamic Interpretation. *Geotecton.* **2018**, *52*, 225–239. [[CrossRef](#)]